Human mesenchymal stromal cells response to biomimetic octacalcium phosphate containing strontium

Always Be Ready for What's Next with

Patient SafetyNet™*

Multiple studies over 10 years at Dartmouth-Hitchcock Medical Center have shown improved clinical outcomes and reduced cost of care.

0
preventable deaths or brain damage due to opioid-induced respiratory depression in monitored patients over 10 years[1]

↓50%
approximate reduction in ICU transfers[2]

↓60%
approximate reduction in rapid response team activations[2]

↓$7 Million
annual cost savings[3]

Masimo SET® is used to monitor over 200 million patients a year.[4]

- Masimo SET® has been shown in more than 100 independent and objective studies to outperform other pulse oximetry technologies[5]
- Radius PPG™ tetherless pulse oximetry allows you to monitor patients from outside the room and beyond
- Remote patient monitoring at central view stations
- Real-time data and alarm notifications on clinicians' smartphones with Replica™

[1] McGrath S et al. *J Patient Saf.* 2020 14 Mar. DOI: 10.1097/PTS.0000000000000696. [2] McGrath S et al. *The Joint Commission Journal on Quality and Patient Safety.* 2016 Jul;42(7):293-302. [3] Taenzer A et al. *Anesthesia Patient Safety Foundation Newsletter.* Spring-Summer 2012. [4] Estimate: Masimo data on file. [5] Published clinical studies on pulse oximetry and the benefits of Masimo SET® can be found on our website at http://www.masimo.com. Comparative studies include independent and objective studies which are comprised of abstracts presented at scientific meetings and peer-reviewed journal articles. *The use of the trademark Patient SafetyNet is under license from University HealthSystem Consortium.

For professional use. See instructions for use for full prescribing information, including indications, contraindications, warnings, and precautions.

Masimo

Click here to learn more >>

PLCO-004854/PLMM-12012A-0321
PLLT-11195B-0121

Society For Biomaterials

Human mesenchymal stromal cells response to biomimetic octacalcium phosphate containing strontium

Zeinab Tahmasebi Birgani,[1] Angad Malhotra,[1,2] Clemens A. van Blitterswijk,[1,2] Pamela Habibovic[1,2]

[1]Department of Tissue Regeneration, MIRA Institute for Biomedical Technology and Technical Medicine, University of Twente, P.O. Box 217, Enschede, 7500 AE, The Netherlands
[2]MERLN Institute for Technology-Inspired Regenerative Medicine, Maastricht University, P.O. Box 616, Maastricht, 6200 MD, The Netherlands

Received 9 October 2015; revised 15 March 2016; accepted 21 March 2016
Published online 9 April 2016 in Wiley Online Library (wileyonlinelibrary.com). DOI: 10.1002/jbm.a.35725

Abstract: The incorporation of bioinorganics into synthetic biomaterials is a promising approach to improve the biological performance of bone graft substitutes, while still retaining their synthetic nature. Among these bioinorganics, strontium ions (Sr^{2+}) have reported enhanced bone formation, and a reduced risk of bone fractures. While previous results have been encouraging, more detailed studies are needed to further develop specific applications. This study demonstrates the effects of Sr^{2+} on the osteogenic differentiation of human mesenchymal stromal cells (hMSCs) when introduced as either a dissolved salt, or incorporated into biomimetic calcium phosphate (CaP) coatings. Upon attachment, hMSCs seeded in the presence of higher Sr^{2+} concentrations presented with a more elongated shape as compared to the controls without Sr^{2+}. Both Sr^{2+} as a dissolved salt in the medium, or incorporated into CaP coatings, positively influenced hMSC alkaline phosphatase (ALP) activity in a dose-dependent manner. At the mRNA level, the expression of osteogenic markers ALP, bone sialoprotein, bone morphogenetic protein 2, osteopontin, and osteoclacin were increased in the presence of Sr^{2+}, independent of the delivery method. Overall, this study demonstrates the positive effects of strontium on the osteogenic differentiation of human MSCs, and supports the use of strontium-incorporated CaPs for bone regeneration applications. © 2016 Wiley Periodicals, Inc. J Biomed Mater Res Part A: 104A: 1946–1960, 2016.

Key Words: bioinorganics, strontium, calcium phosphate coatings, osteogenic differentiation, human mesenchymal stromal cells

How to cite this article: Tahmasebi Birgani Z, Malhotra A, van Blitterswijk CA, Habibovic P. 2016. Human mesenchymal stromal cells response to biomimetic octacalcium phosphate containing strontium. J Biomed Mater Res Part A 2016:104A:1946–1960.

INTRODUCTION

Despite advances in orthopedic and dental surgery, the clinical management of bone defects continues to present challenges.[1] While autograft remains the gold standard for treating bone defects, issues such as limited quantity, donor site morbidity, and the requirement for an additional surgical site continue to encourage research into alternatives.[2] Synthetic bone graft substitutes have provided promising results to date, with calcium phosphates (CaPs) maintaining interest[2] due to their chemical similarities to the mineral phase of bone, being itself a nonstoichiometric carbonated apatite.[3] Despite this, the performance of synthetic bone grafts remains inferior to autograft. Several attempts have been made to improve the bone healing capacity of CaPs,[4] including combining them with growth factors,[5–7] cells[5,8,9] and inorganic additives.[10–12] The incorporation of inorganic additives such as magnesium (Mg^{2+}), copper (Cu^{2+}), strontium (Sr^{2+}), and fluoride (F^-) into synthetic bone grafts, is gaining popularity as these additives may directly induce changes in cells, for example via ion channels, potentially functioning as "synthetic growth factors." The potential role of these bioinorganics in bone tissue, and their effects on bone formation, are comprehensively summarized by Habibovic and Barralet,[13] Yang *et al.*,[4] and Boanini *et al.*[10]

While many elements have been shown to influence bone regeneration, the role of strontium is particularly interesting due to its relatively high presence within healthy bone. Approximately 98% of the strontium within the body is found within bone, with its quantity being positively correlated to the compressive strength of bone.[13] Strontium ranelate is currently used for treatment and management of osteoporotic bone,[14–17] with its use reported to reduce the

Additional Supporting Information may be found in the online version of this article.
Correspondence to: P. Habibovic; e-mail: p.habibovic@maastrichtuniversity.nl
Contract grant sponsor: Dutch Ministry of Economic Affairs, Agriculture and Innovation
Contract grant sponsor: The Netherlands Science Organization (NWO); contract grant number: 015.008.039

risk of fracture in postmenopausal osteoporotic bone,[14] and increase bone mineral density.[15]

To date, several studies have investigated the effects of local Sr^{2+} delivery on osteogenesis and bone formation. Promising results have been obtained when strontium was incorporated into synthetic bone grafts, including bioactive glasses,[18–20] titanium implants,[21,22] calcium silicates,[23] and CaPs.[1,11,24–30] *In vitro* studies have previously demonstrated that strontium incorporation into CaPs resulted in a dose-dependent effect on osteoblast and osteoclast growth and activity.[11,24–27] This effect has also been demonstrated using ovariectomized rats, where the ion release from Sr^{2+}-doped CaPs resulted in increased new bone formation[28] and improved osseointegration.[29]

While the addition of strontium ions to CaP bone graft substitutes has provided positive results to date, a deeper understanding of the mechanisms and function of strontium is still lacking. Such information is needed to convert this potential into applicable products. To further elucidate the specific role of strontium in bone healing, this study investigated the effect of Sr^{2+} on hMSCs in two conditions. In the first condition, Sr^{2+} ions were delivered to the cells as a dissolved salt, in order to understand its direct effect on hMSCs. In comparison, and with the aim to assess a degradable CaP as a delivery vehicle for this ion, the second condition used a two-step biomimetic approach to incorporate Sr^{2+} at varying concentrations into crystalline CaP coatings, which were deposited on titanium substrate. For both conditions, cell responses were studied using proliferation and osteogenic differentiation marker expression, and changes in hMSC morphology. Overall, this study was undertaken to elucidate the specific mechanisms of strontium-induced osteogenesis, and therefore, improve the efficacy of CaPs as bone graft substitutes

MATERIALS AND METHODS

Coating preparation

Commercially pure Titanium (cp Ti grade 4) was used as a substrate for the CaP coatings. The Ti sheet was cut into 1×1 cm^2 pieces and grit-blasted using alumina beads with a diameter of 250 μm to reach a Ra roughness of 1.3 ± 0.1 μm.

A 2-step biomimetic coating approach was used to prepare the coatings, as previously described.[11,31] Briefly, the surface of the Ti plates were coated with a thin amorphous CaP layer by vertical immersion in a supersaturated simulated body fluid (SBF) for 24 h at 37°C. This solution, containing NaCl, $CaCl_2.2H_2O$, $MgCl_2.6H_2O$, $NaHCO_3$, and $Na_2HPO_4.2H_2O$ salts (Sigma, Table I) was prepared under mildly acidic conditions by dissolution of CO_2 gas. The pre-calcified Ti plates were then immersed for 48 h at 37°C in a calcium phosphate solution (CPS) containing NaCl, $CaCl_2.2H_2O$, and $Na_2HPO_4.2H2O$ salts (Sigma, Table I) that was buffered at pH 7.4 by addition of tris-hydrozymethylaminomethane (Tris) and 1*M* HCL (Sigma). A stock solution of strontium acetate (Sigma) in a Tris buffer (pH = 7.4) with concentration of 100 m*M* was prepared. To incorporate strontium into CaP coatings, appropriate volumes of Sr^{2+} stock solution were combined with the CPS solution to reach varying concentrations of Sr^{2+} in CPS (0, 10, and 1000 μ*M*). The CPS solution was refreshed after 24 h. The coatings were then washed three times with MilliQ water and dried overnight at 37°C in an air oven.

TABLE I. Ionic Content of Concentrated SBF and CPS Solutions used for Preparation of the Coatings

Solution	Na^+	Mg^{2+}	Ca^{2+}	Cl^-	HPO_4^{2-}	HCo^{3-}
Concentrated SBF	733.5	7.5	12.5	720	5	21
CPS	140	0	4	144	2	0

Coating characterization

The chemistry of the mineral phase was characterized by Fourier transform infrared spectroscopy (FTIR, Perkin-Elmer Spectrum 1000) and X-ray diffraction (XRD, Miniflex, Rigaku). The morphology of the mineral films, and the presence and distribution of calcium, phosphorus, and strontium were investigated scanning electron microscopy (SEM, XL-30 ESEM-FEG, Philips), coupled with energy dispersive X-ray spectroscopy analyzer (EDS, EDAX, AMETEK Materials Analysis Division). Quantification of the data was achieved using the TEAM™ EDS V2.2 software provided by the EDS manufacturer. The Ca/P, Sr/P, (Ca + Sr)/P, and Sr/Ca ratios were calculated upon analysis.

Additionally, the coatings were dissolved in ultrapure nitric acid and the Sr^{2+} content of the coating was measured using inductively coupled plasma mass spectrometry (ICP-MS, Agilent 7700 ICP-MS, Agilent Technologies).

Cell subculture

hMSCs were isolated from bone marrow aspirates (5–20 mL) obtained from 2 donors after written informed consent. Isolation procedure and full characterization of the cells have been described previously.[32,33] In short, aspirates were resuspended using 20 G needles, plated at a density of 5×10^5 cells per cm^2, and cultured in proliferation medium [consisting of α-MEM (Gibco) supplemented with 10% fetal bovine serum (Lonza), 2 m*M* L-glutamine (Gibco), 0.2 m*M* ascorbic acid (Sigma), 100 U mL^{-1} penicillin and 100 μg mL^{-1} streptomycin (Gibco), and 1 ng ml^{-1} rhbFGF (AbD-Serotec)]. The medium was refreshed every 2–3 days. Cells were harvested at ~80% confluency for subculture until they reached passage 3.

Cell culture

In the first step of cell culture, hMSCs of passage 3 from the 2 donors were seeded on treated tissue culture plates (TCPs) at a density of 10,000 cells/cm^2 [for DNA, alkaline phosphatase (ALP), and qPCR assays] or at 2500 cells/cm^2 (for imaging cell morphology) in ~50 μL of basic medium [α-MEM (Gibco) supplemented with 10% fetal bovine serum (Lonza), 2 m*M* L-glutamine (Gibco), 0.2 m*M* ascorbic acid (Sigma), 100 U ml^{-1} penicillin and 100 μg ml^{-1} streptomycin (Gibco)]. After seeding, 1 mL of either basic or osteogenic medium [basic medium supplemented with 10 n*M*

dexamethasone (Sigma)] was added to each well. Appropriate volumes of Sr^{2+} stock was added to each well to reach Sr^{2+} concentrations of 0, 10, and 1000 μM in cell culture medium. The medium was refreshed every 2–3 days.

In parallel, hMSCs of two donors were cultured on coated Ti plates. CaP coatings were sterilized with ethanol prior to cell culture. To sterilize, the samples were placed in a sterile nontreated well plate and washed three times with 70% ethanol followed by 15 min of drying inside the flow cabinet after each washing step. In the last step of sterilization, 100% ethanol was added to the samples and allowed to evaporate in the flow cabinet for at least 2 h. The plates were then washed twice with sterile PBS, followed by an overnight incubation in a 5% CO_2 humid atmosphere at 37°C after the addition of 1 mL basic medium. hMSCs of passage 3 from 2 donors were seeded on the coated Ti plates at a density of 10,000 cells/cm^2 (for DNA, ALP, and qPCR assays) or 2500 cells/cm^2 (for imaging cell morphology) in ~50 μL of basic medium and allowed to attach to the coatings for 4 h, after which 1 mL of either basic or osteogenic medium was slowly added to each well. The medium was refreshed every 2–3 days. Cell medium was collected at each refreshment point and concentrations of Ca and Sr in basic cell medium were then measured using ICP-MS, at each refreshment point up to 7 days.

Cell morphology

At day 1 after cell seeding, the cells cultured on TCPs and CaP coatings were washed with PBS and fixed with a buffer of 4% paraformaldehyde (pH = 7.4) for 30 min. The cells cultured on TCPs and CaP coatings were then permeabilized with 0.1% Triton X-100 in PBS solution for 10 min, washed with PBS and blocked for 30 min in a blocking solution (2% bovine serum albumin and 0.1 v/v% Tween 20 in PBS). Subsequently, Alexa Fluor 594 antibody (Invitrogen) diluted in blocking buffer was added to the cells to stain the cell cytoskeleton, and incubated at room temperature in dark for 1 hour. After incubation, cells were washed with PBS, and DAPI antibody (Sigma-Aldrich/Fluka) diluted in PBS was added for 10 min. The cells were then washed with PBS and imaged using a fluorescent microscope (E600, Nikon; the data is not shown for cells cultured on CaP coatings).

Six pairs of immunofluorescent images obtained in blue and red channels (for Dapi and Phalloidin antibodies, respectively) were used for quantifying cell shape parameters. The data was analyzed in CellProfiler software as was described previously[34] and cell area and eccentricity parameters were selected to assess the changes in cell morphology upon introduction of Sr^{2+}. Cell area shows the total number of pixels located in the cell area. Eccentricity shows morphological elongation and measures the deviation of a conic section from a circle, with eccentricity being equal to zero for a circle and one for a parabola.[35]

After fixation, the cells cultured on CaP coatings were also dehydrated by addition of alcohol series (70, 80, 90, and 100%, 30 min per concentration) and dried using a critical point drier (CPD 030, Balzers). The samples were then gold sputtered and imaged using SEM. Two independent experiments with $n = 2$ for each condition were performed.

DNA content and ALP activity quantification

Total DNA was assessed with CyQuant Cell Proliferation Assay kit (Invitrogen). After 3 freeze/thaw cycles at −80°C, 500 μL lysis buffer (lysis buffer provided in the kit diluted in a buffer of NaCl-EDTA solution) was added to each well. The samples were ultra-sonicated and incubated at room temperature for 1 h. After centrifugation, 100 μL of the supernatant was mixed with the same volume of CyQuant GR dye in a 96 well microplate and incubated for 15 min. Fluorescence measurements for DNA quantification were done at excitation and emission wavelengths of 480 and 520 nm, respectively, using a spectrophotometer (Perkin Elmer). ALP activity in the cultures was measured using a CDP-star kit (Roche Applied Science); 10 μL of the supernatant was mixed with 40 μL CDP-star reagent in a 96 well microplate and incubated for 30 min. After incubation, chemiluminescence measurements were completed at 466 nm. Results of the DNA assays are presented based on average μg of DNA detected in each condition. Results of ALP activity were normalized per DNA content of each culture and presented as the average of normalized ALP activity per μg of DNA for each condition. Two independent experiments with $n = 3$ for each condition were performed for DNA and ALP analyses, and the results of one representative experiment are presented here.

RNA extraction and gene expression (qPCR) assay

Total RNA was isolated by using a NucleoSpin® RNA II isolation kit (Macherey Nagel) for cells cultured on TCPs and in combination with NucleoSpin® RNA II isolation kit and Trizol method, in accordance with the manufacturer's protocol. RNA was collected in RNAse-free water and the total concentration was measured using nano-drop measurement equipment (ND1000 spectrophotomer, Thermo Scientific). The cDNA of the cultures were then prepared using an iScript kit (Bio-Rad) according to the manufacturer's protocol and diluted 10 times in RNAse-free water to be used for quantitative real-time PCR (qPCR). The qPCR measurements were completed using Bio-Rad equipment using Syber green I master mix (Invitrogen) and the primer sequences (Sigma), which are listed in Table II. Expression of the osteogenic marker genes were normalized to GAPDH levels and fold inductions were calculated by using ΔΔCT method. hMSCs cultured on TCPs in basic medium for 7 days were used as calibrator. Two independent experiments with $n = 3$ for each condition were performed for the qPCR analysis, and the results of one representative experiment are presented here.

Statistical analysis

Statistical comparisons were performed using One-way Analysis of Variance (ANOVA) followed by a Tukey's multiple comparison *post-hoc* test. Error bars indicate one

TABLE II. Primer Sequence of the Osteogenic Genes Investigated

Gene	Primer Sequences
GAPDH (housekeeping gene)	5′-CCATGGTGTCTGAGCGATGT
	5′-CGCTCTCTGCTCCTCCTGTT
Alkaline phosphatase (ALP)	5′-TTCAGCTCGTACTGCATGTC
	5′-ACAAGCACTCCCACTTCATC
Bone morphogenetic protein 2 (BMP2)	5′-GCATCTGTTCTCGGAAAACCT
	5′-ACTACCAGAAACGAGTGGGAA
Bone sialoprotein (BSP)	5′-TCCCGTTCTCACTTTCATA
	5′-CCCCACCTTTTGGGAAAAC
Osteocalcin (OC)	5′-CGCCTGGGTCTCTTCACTAC
	5′-TGAGAGCCCTCACACTCCTC
Osteopontin (OP)	5′-CCAAGTAAGTCCAACGAAAG
	5′-GGTGATGTCCTCGTCTGTA

standard deviation. For all figures, the following p-values apply: $*p < 0.05$.

RESULTS

Mineral film characterization

The 2-step biomimetic technique employed for preparation of the CaP coatings resulted in the formation of a uniform crystalline CaP layer that covered the entire surface of the Ti plates [Fig. 1(a–c)]. The SEM micrographs showed CaP crystals with a plate-like morphology, which formed perpendicular to the surface of the Ti plates. The morphology of the crystals was modified by addition of Sr^{2+} to the initial CPS solution. Sr^{2+}-added CPS solution resulted in smaller and less sharp CaP crystals [Fig. 1(c)].

The presence of the CaP film was confirmed by EDS spectra of the samples, in which sharp peaks of calcium, phosphorous, and oxygen were visible [Fig. 1(d–f)]. EDS elemental maps also showed that Ca and P elements were homogeneously distributed on the surface [Fig. 1(g–l)]. EDS results showed presence of Sr^{2+} in the CaP coatings prepared with a concentration of 1000 μM Sr^{2+} in the CPS solution [Fig. 1(f)]. The EDS strontium elemental maps indicated that Sr^{2+} was homogeneously distributed within the coating [Fig. 1(m–o)]. Quantification of the EDS results indicated an incorporation of approximately 3 at% of strontium into CaP coatings at the highest concentration of Sr^{2+} in CPS solution (Table III). EDS did not detect Sr^{2+} in the coating with low Sr^{2+} incorporation. However, ICP measurements showed the presence of 0.44 and 16.49 mg/l Sr^{2+} in the coatings with low and high incorporation of Sr^{2+} dissolved in HNO_3, respectively (Table III). Comparing the measurement method averages, the ICP measured Sr/Ca at% ratio as 0.01, 0.22, and 10.32, whereas the EDS measured the Sr/Ca at% ratio as 1.75, 1.88, and 8.89, for the OCP Sr0, OCP Sr10, and OCP Sr1000, respectively. Calculation of atomic ratios indicated that the ratio of Sr/P increased from 0.021 to 0.098 by increasing the concentration of Sr^{2+} in CPS solution from 0 to 1000 μM. The Ca/P ratio in these conditions, however, was calculated to be 1.197 and 1.091, respectively. The (Ca + Sr)/P ratios remained constant at ~1.2.

The results of the XRD and FTIR analyses for CaP coatings without and with Sr^{2+} (Fig. 2) were in accordance with data obtained in earlier studies when similar biomimetic coating method was applied.[36–38] The XRD patterns [Fig. 2(a)] of the coatings exhibited peaks at $2\theta = 4.7°$ corresponding to (010) diffraction line and at $2\theta = 25.8°$ corresponding to (002) plane, both typical of triclinic octacalcium phosphate (OCP) crystals. The peaks observed at $2\theta = 9.8°$ and at $2\theta = 27\text{-}28.5°$ can also be attributed to the OCP structure. The broad set of peaks at $\sim 2\theta = 31.5°$ to 32.5° are common for both OCP and apatitic structures. A small shift of $\sim 2\theta = 0.1°$ toward lower degrees was observed in some of the characteristic OCP peaks, when the OCP Sr1000 coating was analyzed. Supporting Information Figure S1 summarizes the position of the main peaks in the XRD patterns of the coatings without and with Sr^{2+} incorporation.

The FTIR spectra of the coatings [Fig. 2(b)] exhibited sharp P-O bands at 560 and 600 cm^{-1}. Moreover, the bands at 906 and 850 cm^{-1} were typical HPO_4^{2-} bands in the OCP phase. Nevertheless the vibration bands observed between 1020 and 1070 cm^{-1} were less sharp and less numerous as compared to phase-pure OCP.[37,38] The small bands observed at 1450 and at 1480 cm^{-1} corresponded to the carbonate group typical of A-B carbonated apatite, suggesting that apart from the OCP, the coating comprised a carbonated apatitic phase. The typical PO_4^{3-} and HPO_4^{-} bands of the coatings prepared in presence of higher concentration of Sr^{2+} were less sharp, suggesting a decrease in crystallinity.

Cell morphology

Cells cultured on TCPs with 1000 μM Sr^{2+} in the basic medium appeared to have a higher aspect ratio compared to cells cultured in basic medium without Sr^{2+} addition, while no apparent differences were observed between the control, and the cells treated with 10 μM of Sr^{2+} [Fig. 3(a–c)].

Quantification of the cell parameters using CellProfiler based on immunofluorescent images showed that the cell area was reduced dose-dependently when Sr^{2+} was added to cell medium. The eccentricity was, however, significantly increased upon addition of Sr^{2+} to cell medium in a dose-dependent manner, confirming increase in elongation of the cells treated with Sr^{2+}.

Similar results were obtained when cells were cultured on OCP coatings. After 1 day, cells cultured on OCP Sr1000 coatings appeared more elongated in their morphology compared with the cells cultured on OCP and OCP Sr10 coatings [Fig. 4(d–f)]. The adhesion points were observed in the cells cultured on all the coatings [Fig. 3(g–i)].

Quantification of the morphology parameters of the cells cultured on CaP coatings based on immunofluorescent images indicated that area of the cells cultured on OCP Sr10 was significantly higher than the area of those cultured on OCP without strontium incorporation. The eccentricity of cells cultured on OCP Sr1000 was also significantly higher than the one of the cells cultured on OCP and OCP Sr10 coatings.

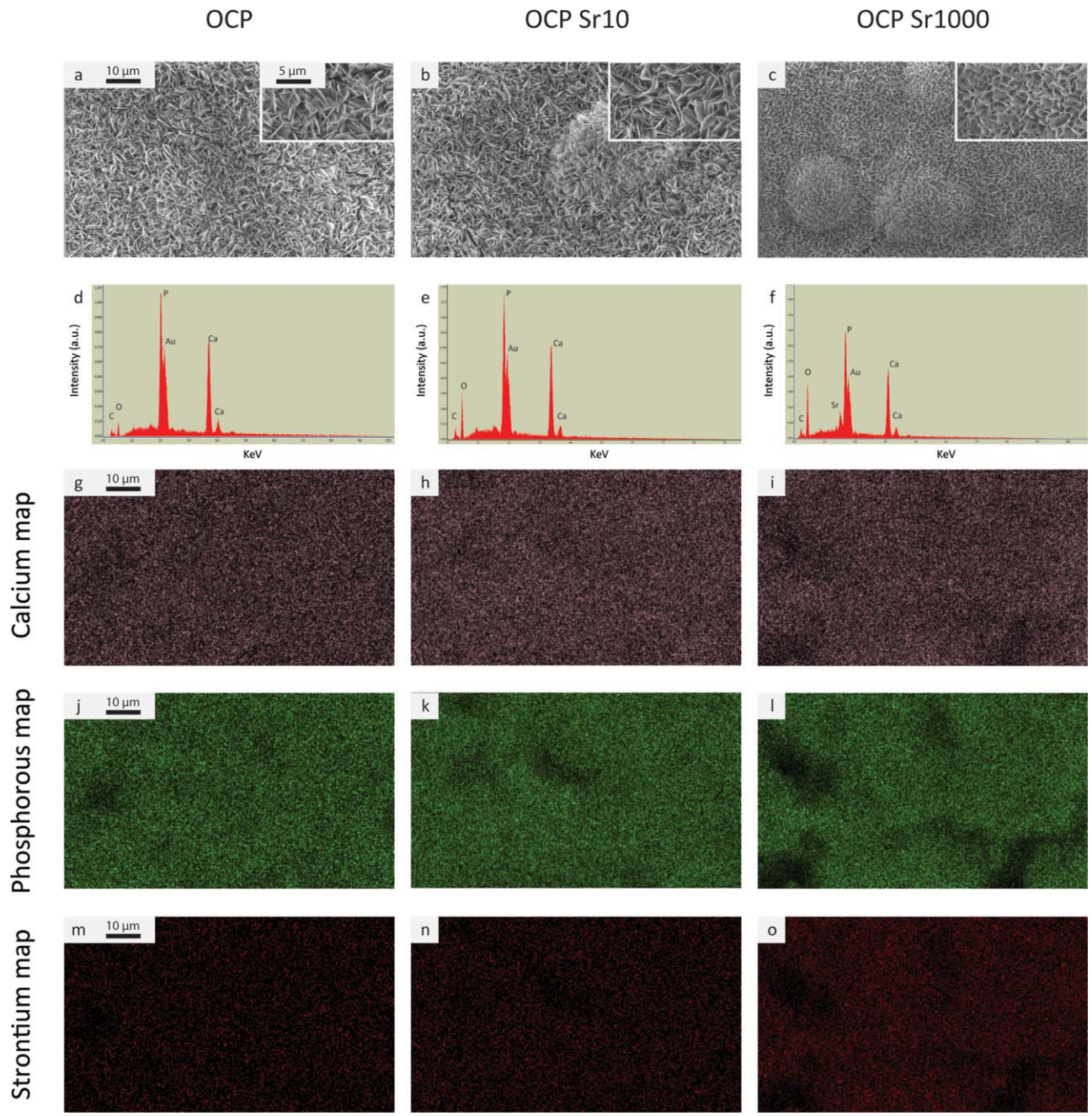

FIGURE 1. SEM images (a,b,c), EDS spectra (d,e,f), Ca elemental map (g,h,i), P elemental map (j,k,l) and Sr elemental map (m,n,o) of OCP, OCP Sr10, and OCP S1000, respectively. A crystalline CaP layer was formed on the surface of Ti plates with a homogenous distribution of all the elements. Presence of Sr^{2+} in higher concentration was detected in EDS spectrum and Sr elemental map of OCP Sr1000. Moreover, the morphology of the coatings changed upon addition 1000 µ Sr^{2+} to CPS solution resulting in smaller and less sharp crystals.

DNA content and ALP activity

At 7 days, the addition of 1000 µ*M* Sr^{2+} to the osteogenic media increased the hMSC DNA content in both donors when cultured on TCPs, however, this increase was only significant in cells of Donor 1. A similar trend was seen when 1000 µ*M* of Sr^{2+} was added to basic media in Donor 1 cultures, but not when cells from Donor 2 were cultured [Fig. 4(a,b)]. The DNA content of the cells did not increase between 7 and 14 days, suggesting the formation of a confluent monolayer before the second time point analysis.

While at 7 days, no significant differences in ALP activity were seen among the conditions, at 14 days, the addition of either 10 or 1000 µ*M* Sr^{2+} to osteogenic media increased the normalized ALP activity of hMSCs. This result was statistically significant for cells of Donor 1, and for 1000 µ*M* in Donor 2 cells [Fig. 4(c,d)].

No differences in DNA content were seen when cells were cultured on coatings for 7 days, however, at 14 days in Donor 2 cells, the incorporation of Sr^{2+} into OCP increased the DNA content, with this result being

TABLE III. Sr Content Measured by EDS and ICP, and Atomic Ratios Quantified Based on EDS Data in CaP Coatings

Sample	Sr Content (at%) Measured by EDS	Sr Content (mg/L) Measured by ICP	Ca/P ratio Measured by EDS	Sr/P ratio Measured by EDS	(Ca + Sr)/P ratio Measured by EDS
OCP Sr0	0.780	0.024	1.197	0,021	1,218
OCP Sr10	0,698	0.444	1,168	0,021	1,189
OCP Sr1000	2.964	16.490	1.091	0,097	1,189

The Sr content in OCP Sr1000 was ~3 at%, whereas the content of both OCP and OCP Sr10 coating was within the background noise, below 1 at%. Increasing the concentration of Sr^{2+} in CPS solution resulted in increasing in Sr/P and a slight decrease in the Ca/P ratios, while (Ca + Sr)/P ratio constantly remained at ~1.2.

statistically significant for both basic and osteogenic media at both incorporation concentrations. This effect, however, was not observed in Donor 1 cells. A difference in proliferation profile was observed between the cells from the two donors, with an increase in DNA content between day 7 and day 14 for the cells from Donor 2 but not for the Donor 1 cells [Fig. 5(a,b)].

At 14 days, the incorporation of Sr^{2+} into OCP at the higher concentration (OCP Sr1000) increased the ALP activity in Donor 1, with this result being statistically significant in both basic and osteogenic media. This effect was also observed in osteogenic medium in Donor 2 cells [Fig. 5(c,d)].

Expression of osteogenic markers at mRNA level

While in basic medium, no significant differences in ALP mRNA expression of cells cultured on TCPs were observed among the conditions at either time point, at 7 days, the addition of 1000 μM of Sr^{2+} to the osteogenic media significantly increased the ALP expression in Donor 1 cells. At 14

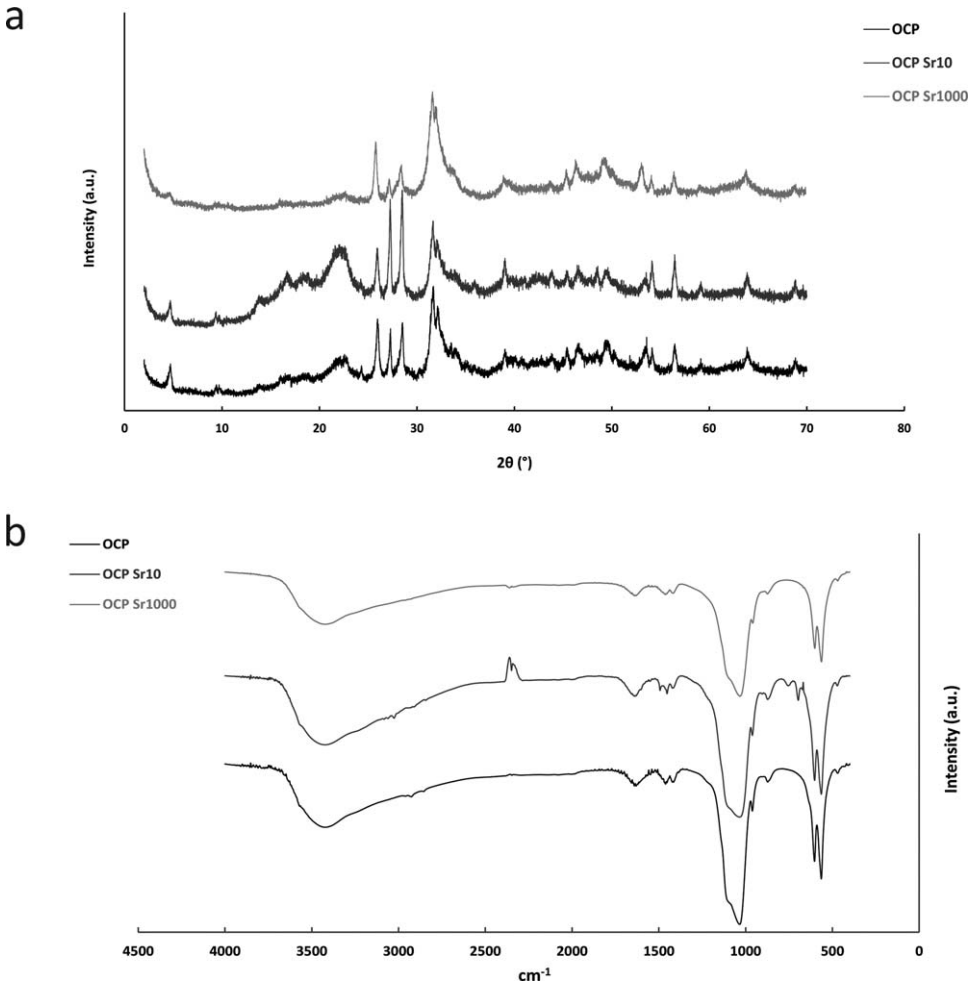

FIGURE 2. XRD patterns (a) and FTIR Spectra (b) of the coatings. The XRD patterns and the FTIR spectra suggested that the coatings predominantly consisted of OCP, with presence of some carbonated apatite. Furthermore, the data suggested that an increase of Sr^{2+} content of the coating led to a limited decrease in crystallinity.

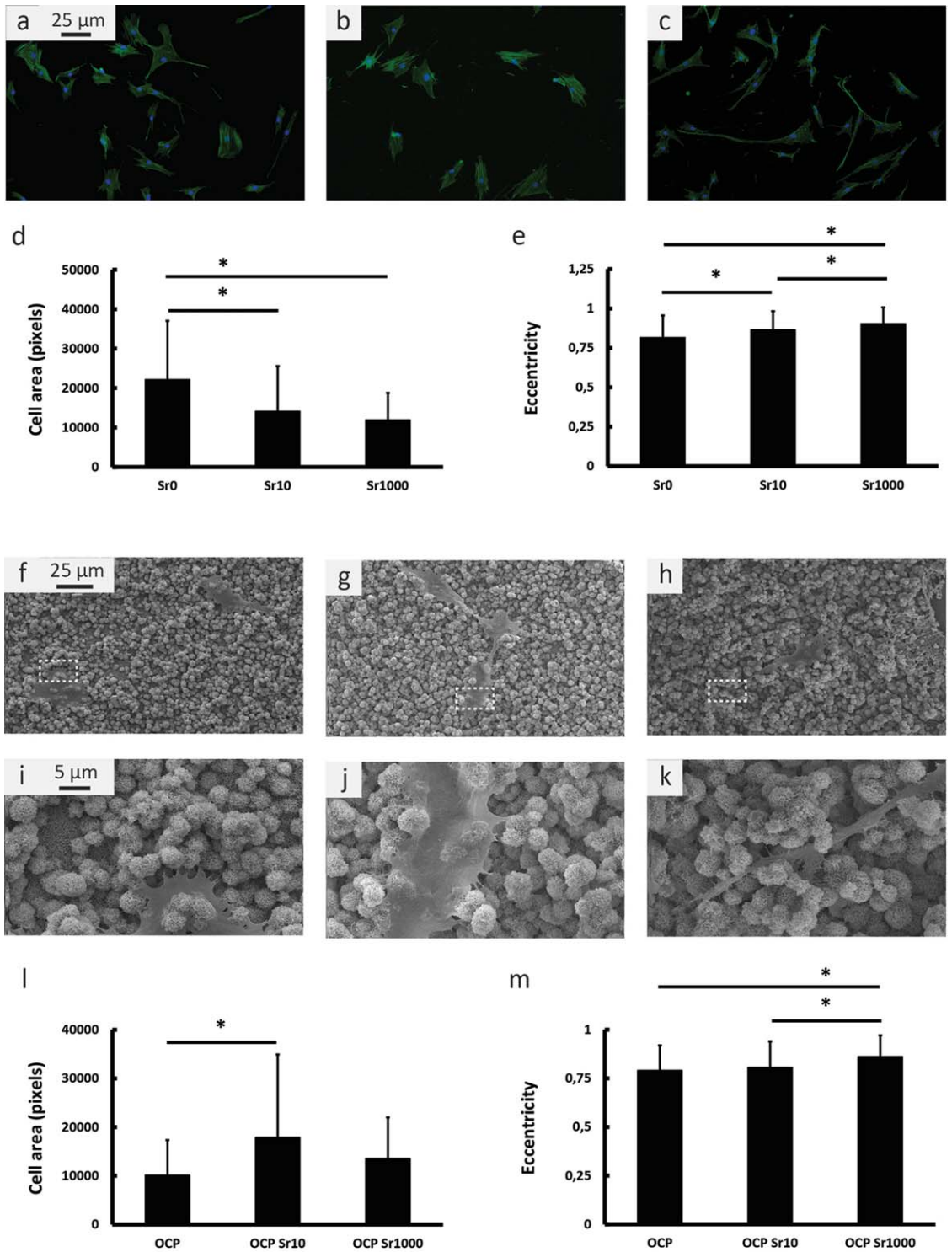

FIGURE 3. Fluorescent microscopy images of the cells cultured for 1 day on TCPs in basic medium without 0 (a), and supplemented with 10 (b) or 1000 (c) µM Sr^{2+}, quantification of cell area (d) and eccentricity (e) of these cells, SEM images of the cells cultured for 1 day in basic medium on OCP (f), OCP Sr10 (g), and OCP Sr1000 (h) coatings with (i–k) magnified images of the areas marked with dashed lines in (f–h) images, respectively, and quantification of cell area (l) and eccentricity (m) of these cells. In fluorescent images, the cells were stained with Dapi (in blue) and Phalloidin (in green) showing cell nuclei and cytoskeleton, respectively. Cells cultured with 1000 µM Sr^{2+} appeared to have a higher aspect ratio compared with cells cultured without Sr^{2+} and with addition of 10 µM Sr^{2}. Cells cultured on OCP Sr1000 coatings were more elongated compared with the cells cultured on OCP and OCP Sr10 coatings. Quantification of eccentricity of the cells confirms these results.

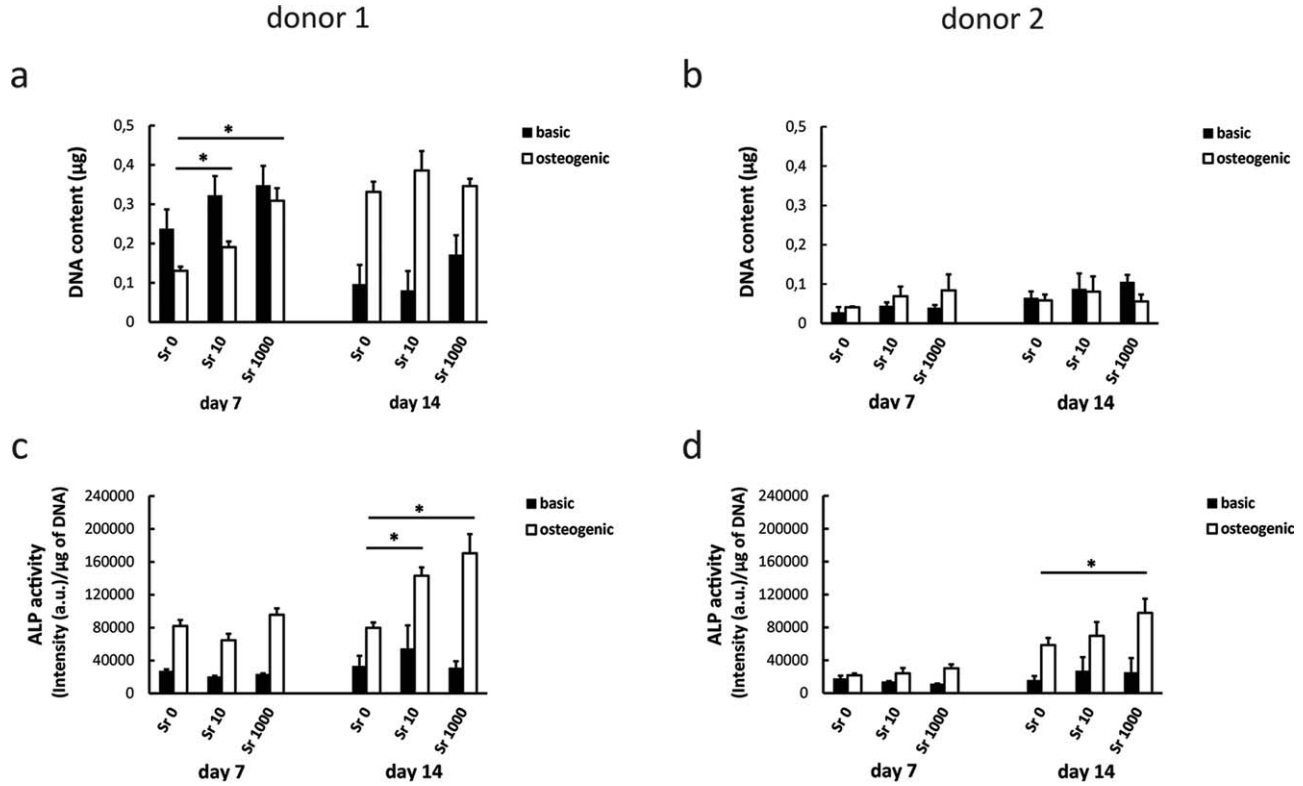

FIGURE 4. DNA content (a, c) and ALP activity (b, d) of hMSCs of, respectively, Donor 1 and Donor 2 cultured on TCPs. Sr^{2+} supplementation in cell culture medium slightly increased the DNA content of the Donor 1 cells at day 7, while no differences were observed for the other conditions. At day 14, addition of Sr^{2+} to osteogenic medium resulted in increasing ALP activity of hMSCs in a dose-dependent manner.

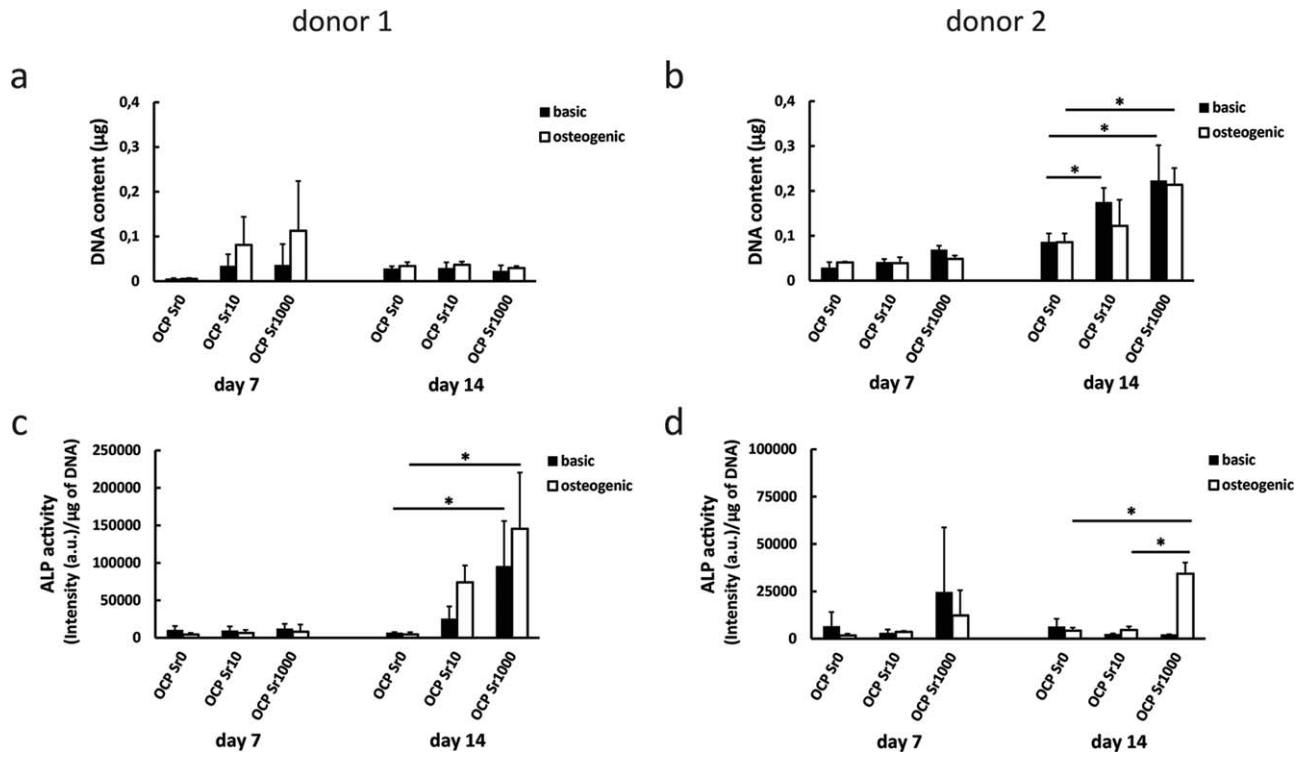

FIGURE 5. DNA content (a, c) and ALP activity (b, d) of hMSCs of, respectively, Donor 1 and Donor 2 cultured on the coatings. At day 14, an increase in DNA content of the cells of Donor 2 was observed upon incorporation of Sr^{2+} into the coatings. At day 14, addition of Sr^{2+} to either medium in cultures of Donor 1 cells and to osteogenic medium in cultures of Donor 2 cells resulted in an increase in ALP activity in a strontium dose-dependent manner.

days, the addition of Sr^{2+} to osteogenic media increased the ALP expression, however, this effect was not consistent between the donors [Fig. 6(a,b)].

At day 7, no differences among the conditions were observed in the bone sialoprotein (BSP) expression when cells were cultured on TCPs in basic medium. However, at day 14, Sr^{2+} supplementation in both basic and osteogenic media resulted in an ascending trend in expression of BSP dependent on Sr^{2+} dose, with a significant effect in osteogenic medium in donor 1 and in basic medium in donor 2 cells [Fig. 6(c,d)].

At days 7 and 14, the addition of Sr^{2+} to basic media only appeared to influence bone morphogenetic protein 2 (BMP2) expression, however, this result was statistically significant only between 0 and 1000 μM in Donor 1, and 10 and 1000 μM in Donor 2. A similar trend was observed in osteopontin (OP) expression in basic media, with significant difference between 10 and 1000 μM in Donor 2 cells. The addition of 1000 μM to osteogenic media significantly increased OP expression in Donor 1, however, this result was not observed in Donor 2 cells [Fig. 6(e,f)].

No significant differences among the conditions were observed in OC expression at 7 days in either medium. At day 14, the addition of Sr^{2+} to both basic and osteogenic media appeared to decrease OC expression in a dose dependent manner in donor 1; however, this result was statistically significant only in osteogenic medium. Unlike in Donor 1 cells, the OC expression by the cells of Donor 2 was significantly increased upon addition of 1000 μM of Sr^{2+} to basic medium at day 14, while no effect was seen in osteogenic medium [Fig. 6(g–j)].

At day 14, hMSCs of donor 1 only, cultured on OCP Sr1000 expressed slightly higher ALP mRNA levels compared with the cells cultured on OCP and OCP Sr10 in basic medium. A similar effect was detected in osteogenic medium, however, this was only significant between OCP and OCP Sr1000. [Fig. 7(a,b)].

Differences in the expression of BSP of cells cultured on different coatings were only observed for Donor 1. At days 7 and 14, incorporation of Sr^{2+} into OCP coatings increased the expression of BSP in basic medium in a dose-dependent manner [Fig. 7(c,d)].

While low BMP2 levels were observed for all conditions in osteogenic medium, at day 14, hMSCs of donor 1 cultured on OCP Sr1000 coating showed higher BMP2 expression compared to the ones cultured on OCP and OCP Sr10 in basic medium. A similar effect, however not significant, was observed in donor 2 as well [Fig. 7(e,f)].

Similar to BMP2, expression of OP was low in osteogenic medium in all the conditions. At day 14, expression of OP in basic medium was higher in OCP Sr1000 coatings compared to OCP and OCP Sr10 in donor 1. A similar, but non-significant effect was observed in donor 2 at similar conditions [Fig. 7(g,h)].

While at 7 days, no significant differences were observed, at day 14, in donor 1, higher OC levels were seen in both media when cells were cultured on OCP Sr1000 coatings compared to OCP and OCP Sr10, however, in basic medium this effect was only significant between OCP Sr1000 and OCP Sr10. In donor 2, OC was upregulated in osteogenic medium in the cells cultured on OCP Sr1000 compared to the cells cultured on OCP and OCP Sr10 [Fig. 7(i,j)].

Ion concentrations in cell medium

Concentrations of Ca^{2+} and Sr^{2+} ions in basic medium up to day 7 were measured using ICP-MS (Table IV). Ca^{2+} content of control cell culture medium, not containing cells or coatings, slightly decreased after 2 days. However, this concentration reached the original values at later time points. A major decrease of >1 μM in Ca^{2+} content of cell medium incubated with CaP coatings cultured with cells was detected after 2 days of culture. Ca^{2+} content of the medium remained constant at this level at later time points. This effect was independent of Sr^{2+} incorporation.

A Sr^{2+} release of $\sim$12 μM was observed in cell medium conditioned with OCP Sr1000 μM after 2 days. The Sr^{2+} release was calculated as $\sim$5 and 2 μM for 4 and 7 days, respectively. The Sr^{2+} release was negligible in the medium conditioned with OCP and OCP Sr10 samples.

DISCUSSION

Among the trace elements within bone mineral, strontium is of particular interest due to its reported osteogenic and antiresorptive effects.[16,17] Pasqualetti *et al*. suggested that, while absolute levels of strontium influence the embryonic mineralization, the actual strontium-to-calcium ratio may also have an important role in the mineralization process.[39] In addition to the chemical interplay, strontium has been suggested to influence cellular responses by affecting the physicochemical properties of the mineral.[11] In this manner, strontium ranelate is thought to prevent osteoporotic fractures via an increase in bone hardness due to the Sr^{2+} ionic substitution.[40,41] To further develop strontium-based treatments, the exact mechanisms of strontium's actions are yet to be fully elucidated.

In this study, a biomimetic approach was taken to prepare strontium-incorporated CaP coatings on Ti substrates. The results indicated that a predominantly crystalline OCP layer formed which was not inhibited by the lower concentration of strontium, though the crystal morphology was influenced at higher strontium concentrations. The presence of strontium was confirmed using EDS and ICP-MS analyses. The decrease in the Ca/P ratio, and increase in the Sr/P ratio, with a constant $(Ca + Sr)/P$ ratio of 1.2 were observed. While the calculated ratio of Ca/P of 1.2 in this study differs to the theoretical OC*P* value of 1.33, this value may have been affected by the semi-quantitative nature of the elemental analysis used. Additionally, the FTIR data indicated the presence of carbonate bands, suggesting the coating formed was not phase-pure. Further, when compared to the coatings formed in absence of Sr^{2+} ions, the small shift to smaller angles was observed in the XRD pattern of OCP Sr1000 coatings, which may be due to the incorporation of strontium ions into the OCP lattice, as shown earlier.[42] This

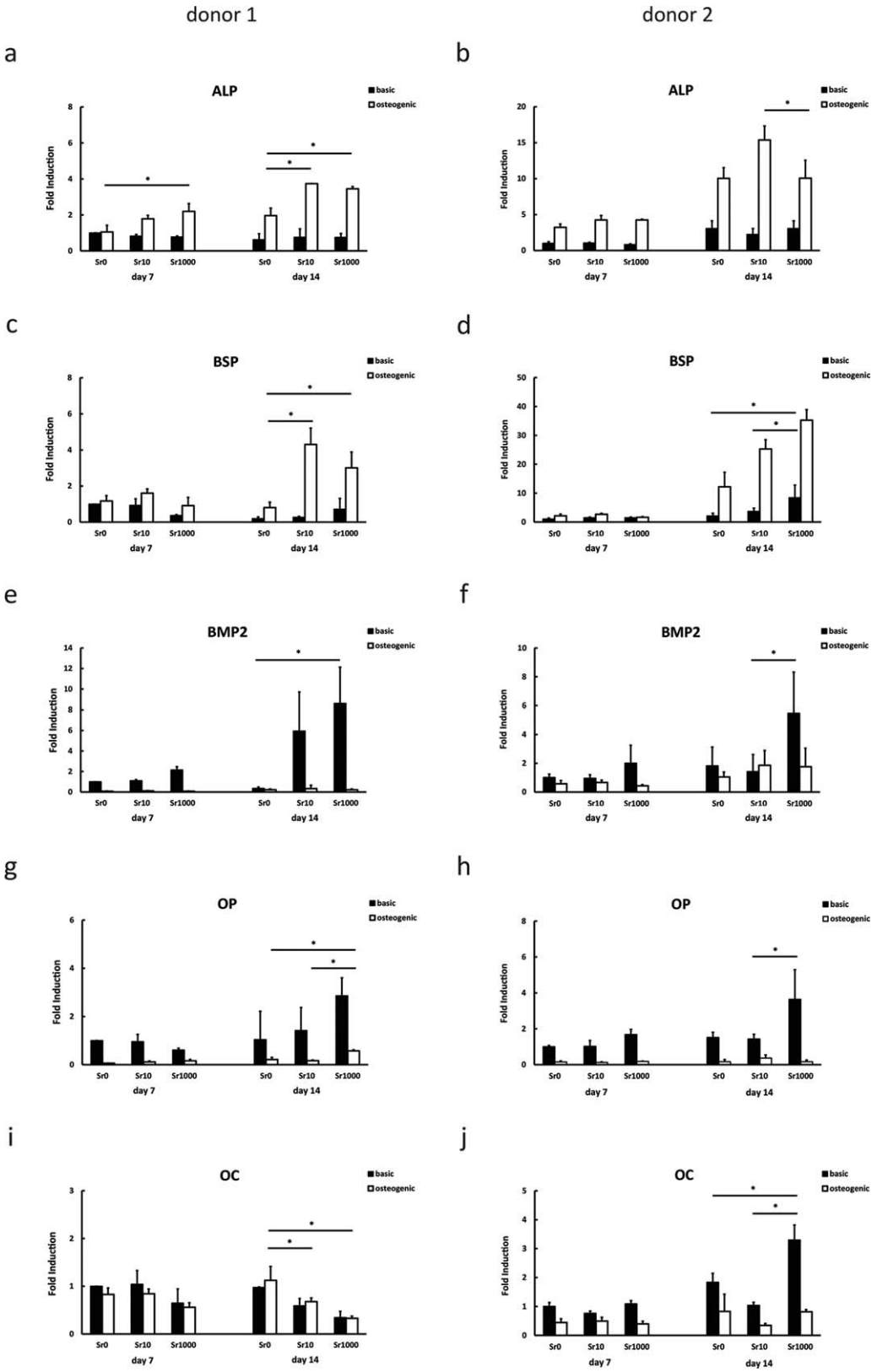

FIGURE 6. mRNA expression of ALP (a,b), BSP (c,d), BMP2 (e,f), OP (g,h), and OC (i,j) by, respectively, hMSCs of Donor 1 and Donor 2 cultured on TCPs. The results are normalized for the mRNA level of GAPDH as a housekeeping gene and calibrated for the mRNA level of each gene of hMSCs cultured in basic medium without supplementation for 7 days. mRNA expression of all the osteogenic markers was altered upon addition of Sr^{2+} to cell culture medium. Sr^{2+} ions generally increased the expression of ALP, BSP, BMP2, and OP, with comparable trends in both donors. Opposing trends were, however, observed in the expression of OC from Donor 1 and Donor 2 cells.

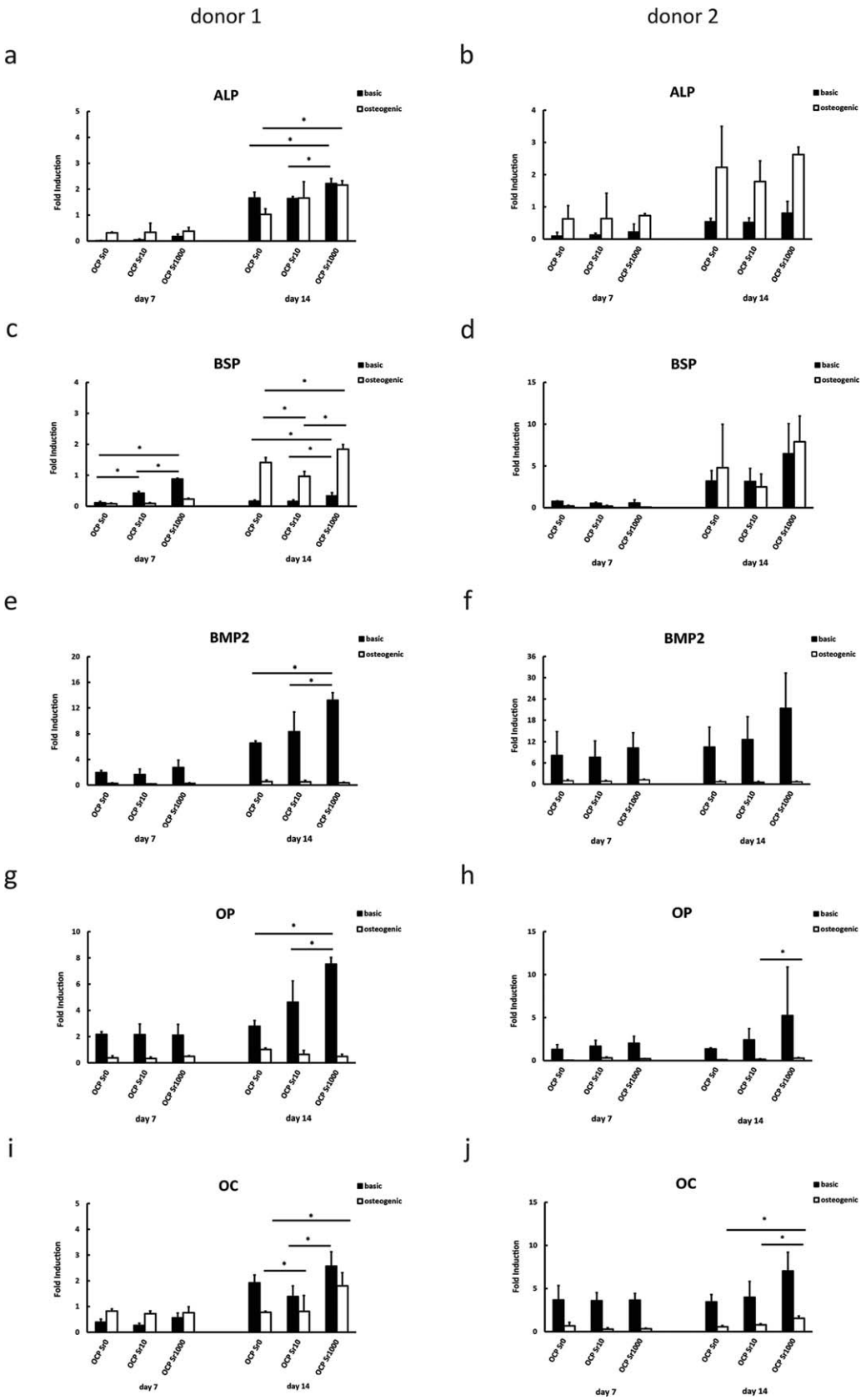

FIGURE 7. mRNA expression of ALP (a,b), BSP (c,d), BMP2 (e,f), OP (g,h), and OC (i,j) by respectively hMSCs of Donor 1 and Donor 2 cultured on CaP coatings. The results are normalized for the mRNA level of GAPDH as a housekeeping gene and calibrated for the mRNA level of each gene in hMSCs cultured in basic medium on OCP coating for 7 days. In general, presence of Sr^{2+} in the CaP coatings positively affected the expression of osteogenic markers. Similar trends were observed in the two donors, with the effects being stronger in Donor 1 cells.

TABLE IV. Ca^{2+} and Sr^{2+} Concentration of Basic Medium Collected During the Culture of hMSCs on CaP Coatings with, as a Control, Basic Medium Without Materials or Cells

			OCP Sr0		OCP Sr10		OCP Sr1000	
Day	Ca^{2+} Content	Sr^{2+} Content	Ca^{2+} Content	Sr^{2+} Content	Ca^{2+} Content	Sr^{2+} Content	Ca^{2+} Content	Sr^{2+} Content
0	1720.50	0.55	1720.50	0.55	172.50	0.55	1720.50	0.55
2	1226.97	0.57	790.99	0.33	769.39	0.48	820.54	12.22
4	1373.85	0.61	773.75	0.34	707.84	0.40	735.46	5.02
7	1757.04	0.69	769.44	0.60	714.88	0.37	770.47	3.22

A decrease of Ca^{2+} concentration was observed after 2 days in all the samples, after which a plateau at about 700 μM was reached. A release of 12, 5, and 3 μM Sr^{2+} after 2, 4, and 7 days, respectively, was detected during cell culture of OCP Sr1000, suggesting dissolution/reprecipitation events occurring on the coating surface.

shift however may also be due to broadening of the diffraction peaks upon addition of the Sr^{2+} or the overall structural change toward a more apatitic phase resulting in modification of the XRD pattern. Therefore, physical entrapment of strontium acetate or another strontium salt into the coating during deposition cannot be fully excluded. Regardless, this data proved the formation of an OCP phase with varying Sr^{2+} content, which was directly dependent on the impregnation concentration of Sr^{2+}.

The results indicated a release of strontium from OCP Sr1000 coatings into basic cell medium at 12, 5, and 3 μ*M* after 2, 4, and 7 days, respectively. A relatively high release of Sr^{2+} after 2 days was accompanied by a pronounced uptake of Ca^{2+} ions from the medium, while at the later time points, the Ca^{2+} concentration remained constant, and release of Sr^{2+} decreased. This may have been due to reprecipitation of a new biological apatite layer formed through dissolution/reprecipitation events occurring on the coating surface.[43] The maximum amount of strontium in the prepared OCP coatings was ~8.9% of the calcium content, which aligns with the percentage reported for a similar method of production.[11] These values are also in the range reported for that of human bone, being 3.9 at%.[44] However, due to ion release via CaP dissolution, it is difficult to relate total incorporated percentage to the actual ion concentration exposed to the cell.

Cytoskeletal components such as actin have been reported to be involved in mediating hMSC proliferation and differentiation toward osteogenic lineage, with early cytoskeletal organization reportedly having a major effect on cell fate.[45] Barradas *et al*.,[46] for example, have shown that the Ca^{2+} induced morphological changes initially occurred in the cytoskeleton as early as after 12 h. Therefore, we have selected a 24 h time point for studying the early morphological organization induced by Sr^{2+}.

The presence of strontium appeared to influence cell shape, with a more elongated morphology observed as compared to cells cultured in absence of strontium. In particular, a dose-dependent effect on cell eccentricity was detected upon increasing strontium concentration. Similar changes in eccentricity have previously been identified as important parameters for interpreting changes in cellular responses.[35] In this study, elongated cells generally corresponded to a higher expression of osteogenic markers at mRNA level. While changes in cell morphology are often considered to relate to cell fate, the morphology corresponding to specific lineages remains uncertain.[45–48] As such, while shape differences were noted in this study, further investigation is needed to provide a more detailed context for these results.

A different trend in the changes in cell area as a function of Sr^{2+} content was observed on TCPs as compared to the CaP coatings. This could in a part be explained by lower levels of Sr^{2+} released from the coatings, as compared to the Sr^{2+} conditioned media. Furthermore, the cell microenvironment provided by the CaP coatings included the presence of other ions, as well as the topographical cues of the substrate surface, which is substantially different from that of the cultures on TCPs.

The addition of strontium appeared to influence the DNA production of hMSCs, which is considered an indicator of cell proliferation. However, these changes were relatively small, being less than two-fold. Sr^{2+} ions have previously shown to increase the proliferation of human osteoblasts,[49] and increase the production of collagen matrix in murine preosteoblast cells.[50] Therefore, enhancing the proliferation and survival of bone forming cells has been proposed as a mechanism in which Sr^{2+} favors bone formation.[4,51] While the results did not reject this hypothesis, this study could did not strongly support this statement.

ALP enzyme activity of hMSCs was generally increased upon exposure to Sr^{2+} ions via both delivery methods, although there was some variation between donors. This finding is consistent with previously reported data.[25–27,49,50]

The effect of strontium on the expression of osteogenic markers at the mRNA level appeared to be dose dependent. This suggests that within the limits of this study, a higher dose of strontium used was favorable. This result aligns with previously published data, in which strontium was reported to have a dose dependent effect on the ALP activity of hMSCs.[27,49,52] Similarly, Brennan *et al*.[49] and Bonnelye *et al*.[16] detected the biologic effects of Sr^{2+} in the form of strontium ranelate on osteogenic markers at a minimum concentration of 1000 μ*M*. Therefore, strontium release and dose should be considered in future strategies.

The expression of osteogenic markers was also highly dependent on the medium used. Generally, expression of BMP2, OP, and OC was higher in basic medium, whereas

ALP and BSP genes were more highly expressed in osteogenic medium. The osteogenic medium used in this study contained 10 n*M* dexamethasone, a concentration previously shows to be optimal for formation of mineralized nodules in human osteoblast precursor cell culture.[53] At this concentration, dexamethasone has also been reported to increase the expression of ALP and RUNX2 of human primary bone cells at mRNA and protein level.[46,53–55] Conversely, evidence exists for the negative effects of glucocorticoids, such as dexamethasone, on bone mineralization, which may lead to lower bone mineral density.[56] Wiontzek *et al*. also demonstrated the inhibitory effects of dexamethasone, in which intracellular Ca^{2+} concentration increased in MG63 shortly after dexamethasone treatment.[57] It appears that in this study, the addition of dexamethasone to cell medium inhibited the regulatory effects of Ca^{2+}, resulting in down-regulation of Ca^{2+}-dependent osteogenic markers including BMP2, OP and OC.[46] Sr^{2+} ions, as a divalent cation similar to Ca^{2+}, may act on similar cellular targets as Ca^{2+}, and similar effects are expected to occur.[46]

Generally, hMSCs cultured on OCP coatings with and without Sr incorporation had a higher expression of BMP2, OP, and OC, and lower expression of ALP and BSP, when compared cells cultured on TCPs in Sr-supplemented media. This is likely due to the regulatory effects of Ca^{2+} ions on BMP2, OP, and OC expression. The Ca^{2+} level in cell medium containing the different coatings was similar and independent of Sr^{2+} incorporation, while the Sr^{2+} concentration differed, which may explain differences in the expression of the osteogenic markers in coatings with and without strontium and suggests the combined effects of both ions. This is further highlighted by the fact that, while the medium concentration of strontium was similar between the OCP Sr1000 and 10 μ*M* Sr^{2+} supplemented media, the hMSC response in these conditions was very different. The expression of BMP2, OP, and OC in OCP Sr1000 was substantially higher than that for the cells cultured with 10 and 1000 μ*M* Sr^{2+} salt, indicating a combinatory effect of strontium and calcium ions on the osteogenic markers, which are known to be Ca^{2+}-dependent. As expected, such an effect was not observed on ALP and BSP expression, even when the presence of strontium in the coatings resulted in upregulating these genes.

It is worth mentioning that the expression of the osteogenic markers at mRNA level does not necessarily translate to production of these proteins. Therefore, the study of the effects of Sr^{2+} addition to the CaPs on production of the osteogenic matrix proteins is recommended for future experiments.

It should be noted that changes in calcium content of the medium in presence of OCP coating are expected to be accompanied by the changes in inorganic phosphate concentration, also known to affect the hMSCs behavior[58] and this effect needs further investigation. Furthermore, possible direct effects of changes in crystal structure upon incorporation of strontium into the coating require further investigation, since the cell fate can be affected by the physical properties of the material surface,[59] such as roughness, microporosity and macroporosity,[60] grain size,[61] and topography.[49,50,62]

CONCLUSION

This study confirms that strontium promotes the osteogenic differentiation of bone marrow derived hMSCs, when introduced to the cells as either dissolved salt or incorporated into CaP coatings. Importantly, the positive effect of strontium appears to synergistically increase when used in combination with CaP coatings. Overall, this study supports the use of Sr^{2+}-incorporated CaPs as potential synthetic bone graft substitutes.

ACKNOWLEDGMENTS

This research forms part of the Project P2.04 BONE-IP of the research program of the BioMedical Materials institute. Authors thank Professor Marc Bohner, Benjamin Andreatta, and Reto Luginbuhl from the RMS Foundation, Switzerland, for collaboration in conducting ICP-MS measurements and critical reading of the manuscript.

REFERENCES

1. Braux J, Velard F, Guillaume C, Bouthors S, Jallot E, Nedelec J, Laurent-Maquin D, Laquerrière P. A New Insight into the Dissociating Effect of Strontium on Bone Resorption and Formation. Acta Biomater 2011;7:2593–2603.
2. Bohner M, Galea L, Doebelin N. Calcium Phosphate Bone Graft Substitutes: Failures and Hopes. J Eur Ceram Soc 2012;32:2663–2671.
3. Bigi A, Cojazzi G, Panzavolta S, Ripamonti A, Roveri N, Romanello M, Noris Suarez K, Moro L. Chemical and Structural Characterization of the Mineral Phase from Cortical and Trabecular Bone. J Inorg Biochem 1997;68:45–51.
4. Yang L, Harink B, Habibovic P. Calcium Phosphate Ceramics with Inorganic Additives. Elsevier; Amsterdam, Netherlands 2011. p 229–312.
5. Vo TN, Kurtis Kasper F, Mikos AG. Strategies for Controlled Delivery of Growth Factors and Cells for Bone Regeneration. Adv Drug Delivery Rev 2012;64:1292–1309.
6. Liu Y, de Groot K, Hunziker EB. BMP-2 Liberated from Biomimetic Implant Coatings Induces and Sustains Direct Ossification in an Ectopic Rat Model. Bone 2005;36:745–757.
7. Malhotra A, Pelletier M, Oliver R, Christou C, Walsh WR. Platelet-Rich Plasma and Bone Defect Healing. Tissue Eng Part A 2014;20:2614–2633.
8. Jäger M, Hernigou P, Zilkens C, Herten M, Li X, Fischer J, Krauspe R. Cell Therapy in Bone Healing Disorders. Orthop Rev 2010;2:79–87.
9. Mooney DJ, Vandenburgh H. Cell Delivery Mechanisms for Tissue Repair. Cell Stem Cell 2008;2:205–213.
10. Boanini E, Gazzano M, Bigi A. Ionic Substitutions in Calcium Phosphates Synthesized at Low Temperature. Acta Biomater 2010;6:1882–1894.
11. Yang L, Perez-Amodio S, Barrère-de Groot FY, Everts V, van Blitterswijk CA, Habibovic P. The Effects of Inorganic Additives to Calcium Phosphate on In Vitro Behavior of Osteoblasts and Osteoclasts. Biomaterials 2010;31:2976–2989.
12. Hoppe A, Güldal NS, Boccaccini AR. A Review of the Biological Response to Ionic Dissolution Products from Bioactive Glasses and Glass-ceramics. Biomaterials 2011;32:2757–2774.
13. Habibovic P, Barralet JE. Bioinorganics and Biomaterials: Bone Repair. Acta Biomater 2011;7:3013–3026.
14. Meunier PJ, Roux C, Seeman E, Ortolani S, Badurski JE, Spector TD, Cannata J, Balogh A, Lemmel EM, Pors-Nielsen S. The Effects of Strontium Ranelate on the Risk of Vertebral Fracture in Women with Postmenopausal Osteoporosis. N Engl J Med 2004;350:459–468.

15. O'donnell S, Cranney A, Wells G, Adachi J, Reginster JY. Strontium Ranelate for Preventing and Treating Postmenopausal Osteoporosis. Cochrane Database Syst Rev 2006;4:CD005326.
16. Bonnelye E, Chabadel A, Saltel F, Jurdic P. Dual Effect of Strontium Ranelate: Stimulation of Osteoblast Differentiation and Inhibition of Osteoclast Formation and Resorption In Vitro. Bone 2008;42:129–138.
17. Marie PJ. Strontium Ranelate: A Dual Mode of Action Rebalancing Bone Turnover in Favour of Bone Formation. Curr Opin Rheumatol 2006;18:S11–S15.
18. Sabareeswaran A, Basu B, Shenoy SJ, Jaffer Z, Saha N, Stamboulis A. Early Osseointegration of a Strontium Containing Glass Ceramic in a Rabbit Model. Biomaterials 2013;34:9278–9286.
19. Gentleman E, Fredholm YC, Jell G, Lotfibakhshaiesh N, O'Donnell MD, Hill RG, Stevens MM. The Effects of Strontium-Substituted Bioactive Glasses on Osteoblasts and Osteoclasts In Vitro. Biomaterials 2010;31:3949–3956.
20. Zhang J, Zhao S, Zhu Y, Huang Y, Zhu M, Tao C, Zhang C. Three-Dimensional Printing of Strontium-Containing Mesoporous Bioactive Glass Scaffolds for Bone Regeneration. Acta Biomater 2014; 10:2269–2281.
21. Andersen OZ, Offermanns V, Sillassen M, Almtoft KP, Andersen IH, Sørensen S, Jeppesen CS, Kraft DCE, Bøttiger J, Rasse M, Kloss F, Foss M. Accelerated Bone Ingrowth by Local Delivery of Strontium from Surface Functionalized Titanium Implants. Biomaterials 2013;34:5883–5890.
22. Zhao L, Wang H, Huo K, Zhang X, Wang W, Zhang Y, Wu Z, Chu PK. The osteogenic Activity of Strontium Loaded Titania Nanotube Arrays on Titanium Substrates. Biomaterials 2013;34:19–29.
23. Lin K, Xia L, Li H, Jiang X, Pan H, Xu Y, Lu WW, Zhang Z, Chang J. Enhanced Osteoporotic Bone Regeneration by Strontium-Substituted Calcium Silicate Bioactive Ceramics. Biomaterials 2013;34:10028–10042.
24. Singh S, Roy A, Lee BE, Ohodnicki J, Loghmanian A, Banerjee I, Kumta PN. A Study of Strontium Doped Calcium Phosphate Coatings on AZ31. Mater Sci Eng A 2014;40:357–365.
25. Zhang W, Shen Y, Pan H, Lin K, Liu X, Darvell BW, Lu WW, Chang J, Deng L, Wang D, Huang W. Effects of Strontium in Modified Biomaterials. Acta Biomater 2011;7:800–808.
26. Boanini E, Torricelli P, Fini M, Sima F, Serban N, Mihailescu IN, Bigi A. Magnesium and Strontium Doped Octacalcium Phosphate Thin Films by Matrix Assisted Pulsed Laser Evaporation. J Inorg Biochem 2012;107:65–72.
27. Capuccini C, Torricelli P, Sima F, Boanini E, Ristoscu C, Bracci B, Socol G, Fini M, Mihailescu IN, Bigi A. Strontium-Substituted Hydroxyapatite Coatings Synthesized by Pulsed-Laser Deposition: In Vitro Osteoblast and Osteoclast Response. Acta Biomater 2008; 4:1885–1893.
28. Thormann U, Ray S, Sommer U, ElKhassawna T, Rehling T, Hundgeburth M, Henß A, Rohnke M, Janek J, Lips KS, Heiss C, Schlewitz G, Szalay G, Schumacher M, Gelinsky M, Schnettler R, Alt V. Bone Formation Induced by Strontium Modified Calcium Phosphate Cement in Critical-Size Metaphyseal Fracture Defects in Ovariectomized Rats. Biomaterials 2013;34:8589–8598.
29. Li Y, Li Q, Zhu S, Luo E, Li J, Feng G, Liao Y, Hu J. The Effect of Strontium-Substituted Hydroxyapatite Coating on Implant Fixation in Ovariectomized Rats. Biomaterials 2010;31:9006–9014.
30. Ni GX, Chiu KY, Lu WW, Wang Y, Zhang YG, Hao LB, Li ZY, Lam WM, Lu SB, Luk KDK. Strontium-Containing Hydroxyapatite Bioactive Bone Cement in Revision Hip Arthroplasty. Biomaterials 2006;27:4348–4355.
31. Patntirapong S, Habibovic P, Hauschk PV. Effects of Soluble Cobalt and Cobalt Incorporated into Calcium Phosphate Layers on Osteoclast Differentiation and Activation. Biomaterials 2009;30:548–555.
32. Fernandes H, Mentink A, Bank R, Stoop R, van Blitterswijk C, de Boer J. Endogenous Collagen Influences Differentiation of Human Multipotent Mesenchymal Stromal Cells. Tissue Eng Part A 2010; 16:1693–1702.
33. Both SK, van der Muijsenberg AJC, van Blitterswijk CA, de Boer J, de Bruijn JD. A Rapid and Efficient Method for Expansion of Human Mesenchymal Stem Cells. Tissue Eng 2007;13:3–9.
34. Carpenter AE, Jones TR, Lamprecht MR, Clarke C, Han Kan I, †, Friman O, Guertin DA, Han Chang J, Lindquist RA, Moffat J, Golland P, Sabatini DM. CellProfiler: image analysis software for identifying and quantifying cell phenotypes. Genome Biol 2006;7: R100–111.
35. Erbil Abaci H, Shen Y, Tan S, Gerecht S. Recapitulating physiological and pathological shear stress and oxygen to model vasculature in health and disease. Sci Rep 2014;4:4951 DOI: 10.1038/srep04951.
36. Habibovic P, Li J, van der Valk CM, Meijer G, Layrolled P, van Blitterswijk CA, de Groot K. Biological Performance of Uncoated and Octacalcium Phosphate-Coated Ti6Al4V. Biomaterials 2005; 26:23–36.
37. Barrère F, Layrolle P, van Blitterswijk CA, de Groot K. Biomimetic Calcium phosphate Coatings on Ti6Al4V: A Crystal Growth Study of Octacalcium Phosphate and Inhibition by Mg^{2+} and HCO_3. Bone 1999;25:107S–111S.
38. Barrère F, Layrolle P, van Blitterswijk CA, de Groot K. Biomimetic Coatings on Titanium: A Crystal Growth Study of Octacalcium Phosphate. J Mater Sci: Mater Med 2001;12:529–534.
39. Pasqualetti S, Banfi G, Mariotti M. The Effects of Strontium on Skeletal Development in Zebrafish Embryo. J Trace Elem Med Biol 2013;27:375–379.
40. Blake GM, Fogelman I. Strontium Ranelate Does not Have an Anabolic Effect on Bone. Bone 2013;9:696–670.
41. Chavassieux P, Meunier PJ, Roux JP, Portero-Muzy N, Pierre M, Chapurlat R. Bone Histomorphometry of Transiliac Paired Bone Biopsies After 6 or 12 Months of Treatment with Oral Strontium Ranelate in 387 Osteoporotic Women: Randomized Comparison to Alendronate. J Bone Miner Res 2014;29:618–628.
42. Guo D, Xu K, Zhao X, Han Y. Development of a Strontium-Containing Hydroxyapatite Bone Cement. Biomaterials 2005;26: 4073–4083.
43. Barrère F, van der Valk CM, Dalmeijer RAJ, van Blitterswijk CA, de Groot K, Layrolle P. In Vitro and In Vivo Degradation of Biomimetic Octacalcium Phosphate and Carbonate Apatite Coatings on Titanium Implants. J Biomed Mater Res Part A 2002;64A:378–387.
44. Pors Nielsen S. The Biological Role of Strontium. Bone 2004;35: 583–588.
45. Treiser MD, Yang EH, Gordonov S, Cohen DM, Androulakis IP, Kohn J, Chen CS, Moghe PV. Cytoskeleton-Based Forecasting of Stem Cell Lineage Fates. Proc Natl Acad Sci USA 2010;107:610–615.
46. Barradas AMC, Fernandes HAM, Groen N, Chai Y, Schrooten J, van de Peppel J, van Leeuwen JPTM, van Blitterswijk CA, de Boer J. A Calcium-Induced Signaling Cascade Leading to Osteogenic Differentiation of Human Bone Marrow-Derived Mesenchymal Stromal Cells. Biomaterials 2012;33:3205–3215.
47. McBeath R, Pirone DM, Nelson CM, Bhadriraju K, Chen CS. Cell Shape, Cytoskeletal Tension, and RhoA Regulate Stem Cell Lineage Commitment. Dev Cell 2004;6:483–495.
48. Dalby MJ, Gadegaard N, Tare R, Andar A, Riehle MO, Herzyk P, Wilkinson CDW, Oreffo ROC. The Control of Human Mesenchymal Cell Differentiation Using Nanoscale Symmetry and Disorder. Nat. Mater 2007;6:997–1003.
49. Brennan TC, Rybchyn MS, Green W, Atwa S, Conigrave AD, Mason RS. Osteoblasts Play Key Roles in the Mechanisms of Action of Strontium Ranelate. Br J Pharmacol 2009;157:1291–1300.
50. Barbara A, Delannoy P, Denis BG, Marie PJ. Normal Matrix Mineralization Induced by Strontium Ranelate in MC3T3-E1 Osteogenic Cells. Metabolism 2004;53:532–537.
51. Saidak Z, Marie PJ. Strontium Signaling: Molecular Mechanisms and Therapeutic Implications in Osteoporosis. Pharmacol Ther 2012;136:216–226.
52. Choudhary S, Halbout P, Alander C, Raisz L, Pilbeam C. Strontium Ranelate Promotes Osteoblastic Differentiation and Mineralization of Murine Bone Marrow Stromal Cells: Involvement of Prostaglandins. J Bone Miner Res 2007;22:1002–1010.
53. Walsh S, Jordan GR, Jefferiss C, Stewart K, Bresford JN. High Concentrations of Dexamethasone Suppress the Proliferation but not the Differentiation or Further Maturation of Human Osteoblast Precursors In Vitro: Relevance to Glucocorticoid-Induced Osteoporosis. Rheumatology 2001;40:74–83.
54. Beresford JN, Joyner CJ, Devlin C, Triffitt JT. The Effects of Dexamethasone and 1,25-Dihydroxyvitamin D on Osteogenic

Differentiation of Human Marrow Stromal Cells In Vitro. Archs Onrl Bid 1994;39:941–947.
55. Langenbach F, Handschel J. Effects of Dexamethasone, Ascorbic Acid and β-Glycerophosphate on the Osteogenic Differentiation of Stem Cells In Vitro. Stem Cell Res Ther 2013;4:117–123.
56. Weiler HA, Wang Z, Atkinson SA. Dexamethasone Treatment Impairs Calcium Regulation and Reduces Bone Mineralization in Infant. Am J Clin Nutr 1995;61:805–811.
57. Wiontzek M, Matziolis G, Schuchmann S, Gaber T, Krocker D, Duda G, Burmester GR, Perka C, Buttgereit F. Effects of Dexamethasone and Celecoxib on Calciumhomeostasis and Expression of Cyclooxygenase-2 mRNA in MG-63 Human Osteosarcoma Cells. Clin Exp Rheumatol 2006;24:366–372.
58. Danoux CBSS, Bassett DC, Othman Z, Rodrigues AI, Reis RL, Barralet JE, van Blitterswijk CIA, Habibovic P. Elucidating the individual effects of calcium and phosphate ions on hMSCs by using composite materials. Acta Biomater 2015;17:1–15.
59. Barradas AMC, Yuan H, van Blitterswijk CA, Habibovic P. Osteoinductive biomaterials: current knowledge of properties, experimental models and biological mechanisms. Eur Cell Mater 2011;21: 407–429.
60. Habibovic P, Yuan H, van der Valk CM, Meijer G, van Blitterswijk CA, de Groot K. 3D microenvironment as essential element for osteoinduction by biomaterials. Biomaterials 2005;26: 3565–3575.
61. Zhang J, Luo X, Barbieri D, Barradas AMC, de Bruijn JD, van Blitterswijk CA, Yuan H. The size of surface microstructures as an osteogenic factor in calcium phosphate ceramics. Acta Biomater 2014;10:3254–3263.
62. Unadkat HV, Hulsman M, Cornelissen K, Papenburg BJ, Truckenmüller RK, Carpenter AE, Wessling M, Post GF, Uetz M, Reinders MJT, Stamatialis D, van Blitterswijk CA, de Boer J. An Algorithm-Based Topographical Biomaterials Library to Instruct Cell Fate. Proc Natl Acad Sci USA 2011;108:16565–1657.